



Development of Oxygen Vacancy-Rich Black TiO₂-Based Electrode Catalyst for Lithium-Oxygen Batteries

Ntakadzeni Madima^{1*}, Thembisile Khumalo¹, Tshimangadzo Munonde², Mpfunzeni Raphulu¹

¹*Advanced Materials Division, Mintek, Private Bag X3015, Randburg, Gauteng Province, South Africa*

²*Institute for Nanotechnology and Water Sustainability, College of Science, Engineering, and Technology, University of South Africa, Florida Science Campus, Roodepoort, 1710, South Africa*

*Corresponding author: NtakadzeniM@mintek.co.za

Abstract

Lithium-oxygen batteries (LOBs) are promising candidates for next-generation energy storage systems due to their high theoretical energy density. However, several challenges currently hinder the practical implementation of these batteries, and addressing these challenges requires the use of innovative electrode materials. In this regard, titanium dioxide-based catalysts are highly desirable as electrode materials due to their excellent catalytic activities and stability. Herein, we develop an oxygen vacancy-rich black titanium dioxide (TiO₂) catalyst as a possible cathode electrode for lithium-oxygen batteries through a chemical reduction method followed by calcination under argon gas. The physicochemical characterization of the synthesized oxygen vacancy-rich black TiO₂ catalyst was compared to its white TiO₂ counterpart using XRD, FTIR, Raman, and BET techniques. The results from electrochemical testing demonstrate that the oxygen vacancy-rich black TiO₂ exhibits excellent electrochemical performance compared to its white TiO₂ counterpart, which was attributed to the improved electrical conductivity and good catalytic activity stimulated by oxygen vacancies. The exceptional electrochemical performance of oxygen-rich vacancy black TiO₂ indicates their potential for use in high-performance lithium-oxygen batteries.

Keywords: White TiO₂; Black TiO₂; Oxygen vacancy; Lithium-oxygen batteries

1. Introduction

As the population grows, there is also a significant rise in the demand for automobiles [1]. Conversely, this has led to substantial environmental impacts because most traditional automobiles are powered by fossil fuels [2]. Therefore, research into renewable energy sources as an alternative to fossil fuels has become crucial [3]. In this context, fostering the progress of electric vehicles (EVs) is a viable solution to tackle this challenge. However, electric vehicles and their energy storage systems necessitate the advancement of high-capacity, long-lasting rechargeable batteries since their driving range and practical use mainly depend on their power battery [4]. Recently, lithium-oxygen batteries (LOBs) have stood out as promising energy storage candidates for next-generation EVs due to their high theoretical energy density (~11,140 Wh kg⁻¹) and higher specific capacity (~3500 mAh g⁻¹) [5,6]. Nonetheless, although some fascinating research has been conducted around LOBs, their development is still in its early stages. Several challenges, such as low round-trip efficiency, short cycle life, sluggish redox kinetics, and instability of electrode materials currently hinder the practical implementation of these batteries [6,7].

Consequently, developing innovative electrode materials with excellent stability, high electrical conductivity, and the ability to support efficient redox kinetics is crucial to overcoming these challenges. Different electrode materials have been developed for over a decade, including noble metals, carbon materials, and transition metals (metal oxides). Amongst these, titanium dioxide (TiO₂) as a metal oxide has been extensively researched as an electrode material due to its affordability, superior catalytic properties, and strong durability [8]. However, pristine TiO₂ has limited electronic and lithium ion conductivity, restricting its widespread use in energy storage applications such as batteries [9,10]. Nonetheless, it has been demonstrated that enhancing the surface properties of TiO₂ through surface engineering and the addition of oxygen vacancies is a practical approach to overcoming the current challenges faced by pristine TiO₂ in battery technology [9,11]. This approach improves TiO₂ electronic and ionic conductivity and alters the surface oxidation state of pristine TiO₂, creating more active sites for oxygen reaction kinetics [12].

Therefore, we develop an oxygen vacancy-rich black TiO₂ catalyst for possible application in LOBs. Using different techniques, we compared the physicochemical and electrochemical characterizations of the synthesized oxygen vacancy-rich black TiO₂ catalyst to its white TiO₂ counterpart. The results demonstrate that oxygen vacancy-rich black TiO₂ exhibits excellent electrochemical performance compared to white TiO₂, attributed to high electrical conductivity and good catalytic activity stimulated by oxygen vacancies. The exceptional

electrochemical performance of oxygen vacancy-rich black TiO₂ catalyst indicates its potential use as a cathode electrode for high-performance LOBs.

2. Experimental section

2.1. Catalyst preparation

White TiO₂ was synthesized by thermal annealing P25 at 450°C for two hours.

The following procedure was followed to synthesize oxygen vacancy-rich black TiO₂: White TiO₂ was mixed with sodium borohydride (NaBH₄) at a molar ratio of 1:1. The mixture was ground to homogeneity using pastel and mortar. Then, the powder was transferred into the crucible and subjected to calcination in a Tube furnace at 450°C under an Argon atmosphere for two hours at a heating rate of 5°C/min. At the end of calcination, the furnace was allowed to cool down to room temperature, and the product was collected and dispersed into 0.1 M hydrochloric acid (HCl) for two hours. Lastly, the sample was washed several times with di-ionized water and ethanol through centrifugation and then dried in an oven at 60°C overnight.

2.2. Catalysts characterizations

X-ray diffraction (XRD) measurements were measured using a MeasSrv D2-205530 diffractometer (Bruker, USA) with CuK α radiation ($\lambda = 1.54056 \text{ \AA}$) in a scan range of 10–80°. Fourier transform infrared resonance (FTIR) analysis was conducted on a Perkin Elmer spectrum 100 spectrometer using the KBr pellet method in the wavenumber ranging from 4000 to 400 cm⁻¹. The PerkinElmer Raman Station 400 benchtop was used for the Raman spectroscopy analysis. N₂ adsorption-desorption experiments were performed at -195°C using a Micromeritics Tristar 3000 surface area and porosity analyzer. The samples were degassed at 150°C for four hours under flowing nitrogen gas.

2.3. Electrochemical measurements

The electrochemical tests were performed on Autolab potentiostat/galvanostat (PGSTAT 302 N model, Metrohm, Swiss instruments) with a standard three-electrode system. A platinum wire (Pt wire) was used as the counter electrode, and Ag/AgCl as the reference electrode. The working electrode was prepared by mixing 10 mg of synthesized catalysts as an active material and 0.05 wt% of the Nafion as a binder. An appropriate amount of 2-propanol and water at the ratio of 3:1 was added dropwise into the mixture and sonicated for 60 minutes to form a homogeneous slurry. The slurry was evenly coated on the glassy carbon electrode and dried at 60°C for one hour. The loading active material for each electrode was about 2 μL . The measurements were done with 0.1M Lithium acetate dihydrate electrolyte solution. Cyclic voltammetry (CV) measurements were carried out using a scan rate of 20 mVs⁻¹ within a potential window of -1.0–1.0 V. The electrochemical impedance spectrum (EIS) was measured in a frequency range of 200 kHz–100 mHz at an amplitude of 10 mV, and liner-sweep voltammetry (LSV) was recorded at a scan rate of 50 mVs⁻¹.

3. Results and discussion

The XRD analysis was conducted to examine the crystal structure of the prepared samples. As displayed in Figure. 1a, both black TiO₂ and white TiO₂ show diffraction peaks at $2\theta = 25.4^\circ, 37.8^\circ, 48.1^\circ, 54.2^\circ, 55.2^\circ, 62.8^\circ, 70.2^\circ,$ and 75.2° corresponding to the (101), (004), (200), (105), (211), (204), (220), and (215) planes of anatase titania (JCPDS Card No. 21-1272) [13]. This shows that black TiO₂ has the same crystal structure as white TiO₂, demonstrating the structural stability of the prepared electrocatalyst [14]. However, black TiO₂ also shows an additional diffraction peak at around $2\theta = 43.2^\circ$, which can be ascribed to impurities of the unreacted NaBH₄ [15]. Moreover, the peak intensity of black TiO₂ is diminished, indicating that the chemical reduction has introduced disorder into the catalyst's original structure by creating defects. These findings demonstrate that chemically reducing TiO₂ leads to a color change from white to black, while the crystal structure remains intact [16].

The FTIR analysis was conducted to understand the chemical bonding species of the as-synthesized catalysts, and the results are presented in Figure. 1b. Both white and black TiO₂ display characteristic bands typically at 400–700 cm⁻¹, indicating the stretching vibration modes of metal oxides (Ti-O and Ti-O-Ti). The transmission intensity of black TiO₂ appears to be lower as compared to white TiO₂ at the range 400–700 cm⁻¹, which can be attributed to the higher concentration of oxygen vacancies in black TiO₂, which causes some of the Ti-O and Ti-O-Ti bonds to be broken. Additionally, the O-H bending vibration modes are linked to the characteristic bands at 1688 and 1524 cm⁻¹, while the bands at approximately 3750 cm⁻¹ are associated with the Ti-OH stretching and wagging modes. A Ti-OH absorption band in black TiO₂ indicates that the OH groups on the disordered black TiO₂ surface have a more varied environment than on the white TiO₂ crystalline surface [17,18].

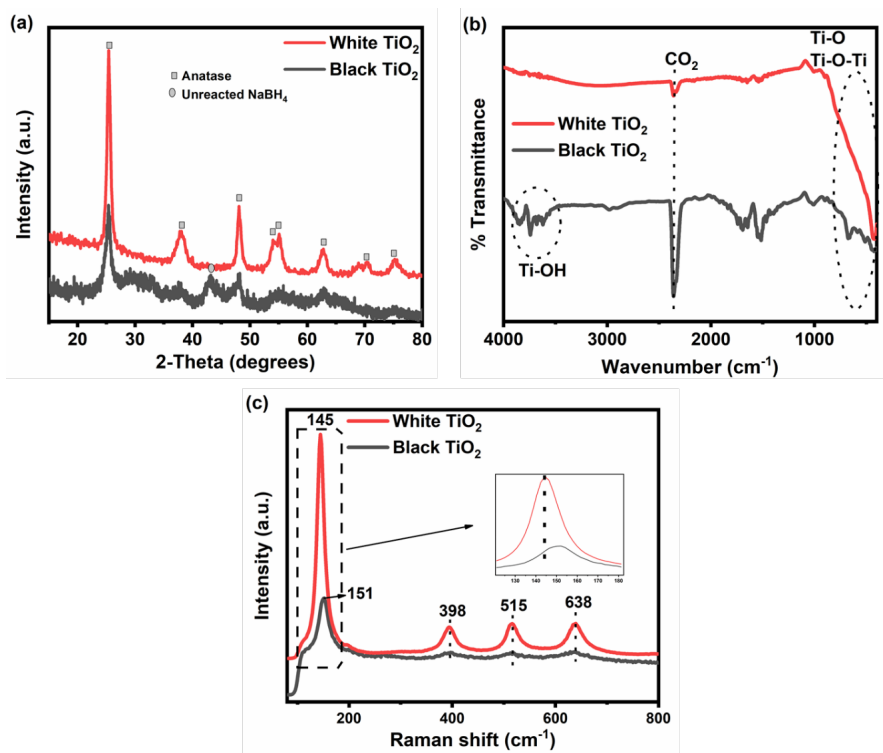


Figure 1. XRD patterns (a), FTIR spectra (b), and Raman spectra (insert is the magnified peak) (c), of white and black TiO₂.

Raman spectroscopy was used to examine the surface structure of the prepared catalysts, and the results are demonstrated in Figure 1c. Both samples show Raman peaks at 145, 398, 515, and 638 cm^{-1} , representing the Eg, B1g, A1g, and Eg modes of the anatase phase, which is consistent with the XRD results. Figure 1c (inserted) shows that black TiO₂ exhibits a blue shift and peak broadening at the sharpest Raman characteristic peak of the Eg mode (145 cm^{-1}) compared to white TiO₂. This shift and broadening are attributed to the introduction of oxygen vacancies on the surface of TiO₂, leading to changes in the Ti-O bond vibration [11,19].

The Nitrogen adsorption-desorption isotherms for white TiO₂ and black TiO₂ can be seen in Figure 2. Both samples exhibit Type-IV isotherm curves with H3 hysteresis loops, suggesting the presence of mesoporous structures (pore diameters ranging from 2 to 50 nm) (Figure 2a) [18]. Furthermore, the specific surface areas were calculated using the standard multi-point BET method. The specific surface areas of white TiO₂ and black TiO₂ were determined to be 147.57 and 105.31 m^2/g , respectively. The reduction in surface area observed in black TiO₂ primarily results from the structural collapse of its porous framework during the chemical reduction process [14]. Additionally, the BJH method (Figure 2b) was utilized to calculate the pore size distributions, revealing average pore sizes of 10.84 nm for white TiO₂ and 12.79 nm for black TiO₂. The porous nature of TiO₂ makes it a suitable cathode electrode catalyst for LOB due to abundant porous channels for the diffusion of oxygen and lithium ions [20].

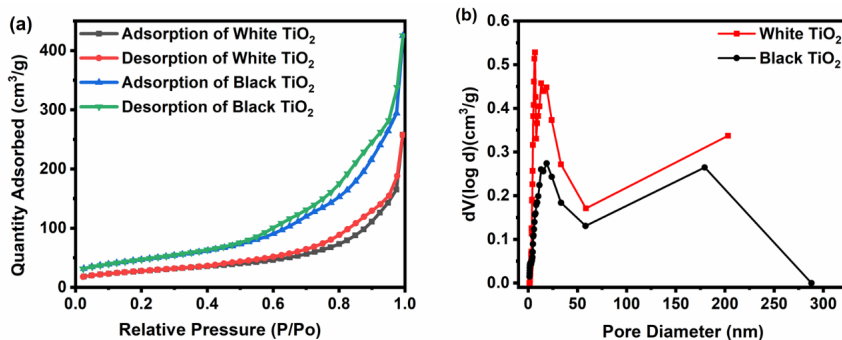


Figure 2. The N_2 adsorption-desorption isotherms (a) and pore size distribution (b) of white and black TiO_2 .

The electrochemical behaviour of the synthesized white TiO_2 and black TiO_2 catalysts was thoroughly analyzed using various electrochemical techniques, including CV, EIS, and LSV, and the results are illustrated in Figure 3. CV tests, as displayed in Figure 3a revealed that white TiO_2 exhibited no discernible reduction/oxidation peaks, indicating relatively poor electrochemical activity. Contrarily, black TiO_2 displayed distinct reduction and oxidation peaks at approximately -0.66 V and 0.32 V, respectively, indicating enhanced electrochemical activities. These peaks were attributed to the improved Li insertion/extraction into anatase TiO_2 [21]. Notably, black TiO_2 exhibited higher current intensity and larger integration areas than white TiO_2 , indicating its ability to generate more discharge products [9].

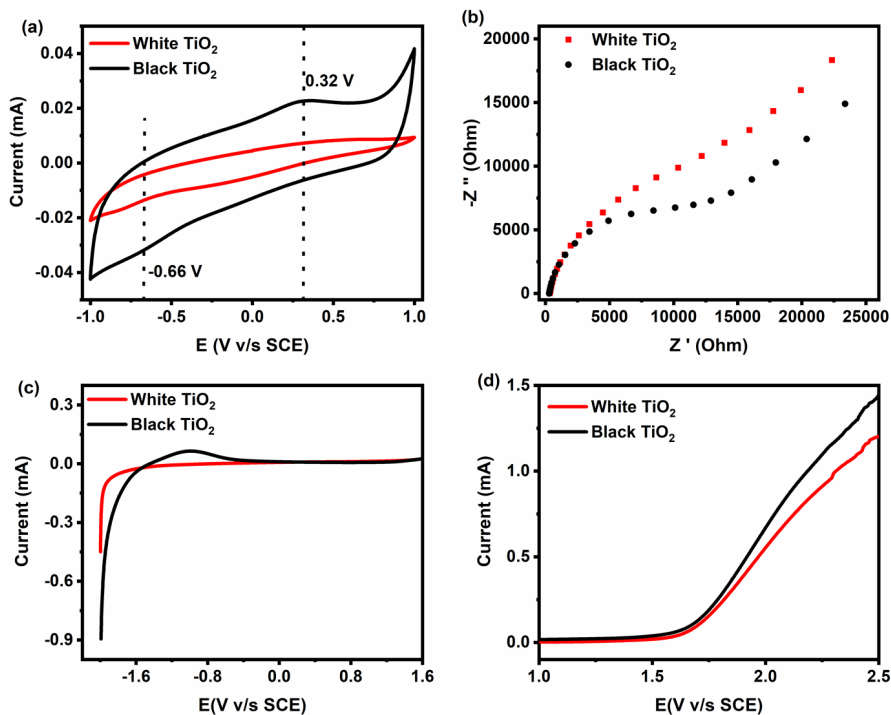


Figure 3. Electrochemical performance: CVs at a scan rate of 20 mVs^{-1} at a voltage window of -1.0 – 1.0 V (a), EIS in a frequency range of 200 kHz – 100 mHz at an amplitude of 10 mV (b), and LSV at a scan rate of 50 mVs^{-1} (c and d), of white and black TiO_2 .

Furthermore, the charge-transfer resistances (R_{ct}) of white TiO₂ and black TiO₂ were investigated using EIS, as depicted in Figure. 3b. Both plots displayed a semicircle followed by an inclined linear segment. Notably, the semicircle diameter of black TiO₂ was significantly smaller than that of white TiO₂, indicating lower charge-transfer resistance in black TiO₂. The solution resistance (R_s) of black TiO₂ was slightly lower than that of white TiO₂, suggesting the ability of Li ions to diffuse from and to the cathode of black TiO₂ than in white TiO₂. This suggests that introducing oxygen defects can effectively reduce the charge-transfer, enhancing the conductivity and rapid transport of lithium ions [22], agreeing with the more porous structure of black TiO₂ observed in the N₂ adsorption-desorption results.

Additionally, LSV was utilized to probe the oxygen reduction reaction (ORR) and oxygen evolution reaction (OER) characteristics of the synthesized catalysts, and the results are presented in Figure. 3(c and d). From the LSV results of ORR (Figure. 3c), the onset potential of black TiO₂ (-1.58 V vs. SCE) was found to be more positive than that of white TiO₂ (-1.89 V vs. SCE), indicating that the black TiO₂ possess higher ORR electrocatalytic activity to enhance the formation of discharge products [23]. Furthermore, LSV results of OER (Figure. 3d) demonstrate that black TiO₂ exhibits a lower OER onset potential than white TiO₂, suggesting its higher electrocatalytic activity towards the OER to decompose the discharge products effectively [24]. Consequently, these results indicate that the black TiO₂ catalyst possesses excellent bifunctional activities towards the ORR/OER to improve the performance of LOBs. This is likely due to the excellent electrical conductivity of black TiO₂ and the efficient transport of electrons resulting from the presence of oxygen vacancies. Based on the analysis of electrochemical activities, it has been established that black TiO₂ demonstrates superior electrochemical performance compared to white TiO₂. This can be linked to oxygen vacancies in black TiO₂, which have led to modifications in the structural and electronic properties of TiO₂, ultimately contributing to its enhanced performance [25].

4. Conclusions

In summary, an oxygen vacancy-rich black TiO₂ catalyst was synthesized through a chemical reduction-assisted calcination method. Various analyses, including XRD, FTIR, Raman, and BET, were conducted to compare the physical properties of black TiO₂ with white TiO₂. The XRD analysis confirmed the anatase phase for both black and white TiO₂. The presence of oxygen vacancies in black TiO₂ was evident from the Raman spectrum. BET analysis indicated the presence of a porous channel, which is advantageous for LOBs as it enables ion transport. Additionally, the study found that the oxygen vacancy-rich black TiO₂ exhibits better electrochemical performance than white TiO₂. The exceptional performance of these oxygen-rich vacancy black TiO₂ underscores their potential as high-performance electrode catalysts in LOBs, offering a promising pathway toward developing more efficient and durable energy storage solutions for the next generation of electric vehicles.

Acknowledgments

The authors appreciate the support from the Advanced Materials Division Catalysis group at Mintek and the Institute for Nanotechnology and Water Sustainability (iNanoWS) of the University of South Africa.

Disclosure of Interests

The authors declare no conflict of interest.

References

- [1] S. Hemavathi, A. Shinisha, A study on trends and developments in electric vehicle charging technologies, *J. Energy Storage* 52 (2022) 105013. <https://doi.org/10.1016/j.est.2022.105013>.
- [2] S.O. Rey, J.A. Romero, L.T. Romero, À.F. Martínez, X.S. Roger, M.A. Qamar, J.L. Domínguez-García, L. Gevorgov, Powering the Future: A Comprehensive Review of Battery Energy Storage Systems, *Energies* 16 (2023). <https://doi.org/10.3390/en16176344>.
- [3] M.K.G. Deshmukh, M. Sameeroddin, D. Abdul, M. Abdul Sattar, Renewable energy in the 21st century: A review, *Mater. Today Proc.* 80 (2023) 1756–1759. <https://doi.org/10.1016/j.matpr.2021.05.501>.
- [4] H. Xia, Q. Xie, Y. Tian, Q. Chen, M. Wen, J. Zhang, Y. Wang, Y. Tang, S. Zhang, High-efficient CoPt/activated functional carbon catalyst for Li-O₂ batteries, *Nano Energy* 84 (2021) 105877. <https://doi.org/10.1016/j.nanoen.2021.105877>.
- [5] Y. Zhang, F. Bai, H. Jiang, T. Zhang, A cascade protection strategy from cathode to anode with high air stability for ultralong life Li-air batteries in ambient conditions, *Energy Storage Mater.* 54 (2023) 508–516. <https://doi.org/10.1016/j.ensm.2022.10.040>.
- [6] Y. Zhou, S. Guo, Recent advances in cathode catalyst architecture for lithium-oxygen batteries, *EScience* 3 (2023) 100123. <https://doi.org/10.1016/j.esci.2023.100123>.

- [7] Q. Qiu, J. Long, P. Yao, J. Wang, X. Li, Z.Z. Pan, Y. Zhao, Y. Li, Cathode electrocatalyst in aprotic lithium-oxygen (Li-O₂) battery: A literature survey, *Catal. Today* 420 (2023) 114138. <https://doi.org/10.1016/j.cattod.2023.114138>.
- [8] S.H. Kang, Y.N. Jo, K. Prasanna, P. Santhoshkumar, Y.C. Joe, K. Vediappan, R. Gnanamuthu, C.W. Lee, Bandgap tuned and oxygen vacant TiO_{2-x} anode materials with enhanced electrochemical properties for lithium-ion batteries, *J. Ind. Eng. Chem.* 71 (2019) 177–183. <https://doi.org/10.1016/j.jiec.2018.11.020>.
- [9] C. Wang, X. Peng, W. Fang, L. Fu, L. Liu, Y. Wu, TiO₂-based cathode with modest oxygen vacancies and defective Ti³⁺ for long-life lithium-oxygen batteries, *Appl. Surf. Sci.* 614 (2023) 156262. <https://doi.org/10.1016/j.apsusc.2022.156262>.
- [10] L. Zhang, X. Bai, G. Zhao, X. Shen, Y. Liu, X. Bao, J. Luo, L. Yu, N. Zhang, A visible light illumination assistant Li-O₂ battery based on an oxygen vacancy doped TiO₂ catalyst, *Electrochim. Acta* 405 (2022) 139794. <https://doi.org/10.1016/j.electacta.2021.139794>.
- [11] G. Wang, W. Gao, Z. Zhan, Z. Li, Defect-engineered TiO₂ nanocrystals for enhanced lithium-ion battery storage performance, *Appl. Surf. Sci.* 598 (2022) 153869. <https://doi.org/10.1016/j.apsusc.2022.153869>.
- [12] T.S. Rajaraman, S.P. Parikh, V.G. Gandhi, Black TiO₂: A review of its properties and conflicting trends, *Chem. Eng. J.* 389 (2020) 123918. <https://doi.org/10.1016/j.cej.2019.123918>.
- [13] Y. Feng, H. Liu, Y. Liu, F. Zhao, J. Li, X. He, Defective TiO₂-graphene heterostructures enabling in-situ electrocatalyst evolution for lithium-sulfur batteries, *J. Energy Chem.* 62 (2021) 508–515. <https://doi.org/10.1016/j.jechem.2021.04.008>.
- [14] S. Wu, X. Li, Y. Tian, Y. Lin, Y.H. Hu, Excellent photocatalytic degradation of tetracycline over black anatase-TiO₂ under visible light, *Chem. Eng. J.* 406 (2021) 126747. <https://doi.org/10.1016/j.cej.2020.126747>.
- [15] X. Luo, A. Rawal, K.F. Aguey-Zinsou, Investigating the factors affecting the ionic conduction in nanoconfined nabh₄, *Inorganics* 9 (2021) 1–10. <https://doi.org/10.3390/inorganics9010002>.
- [16] S. Liu, L. Bao, Q. Jia, X. Qiao, D. Wang, Controllable preparation of black titanium dioxide and its wave-absorbing properties, *Appl. Phys. A Mater. Sci. Process.* 129 (2023) 1–10. <https://doi.org/10.1007/s00339-022-06301-6>.
- [17] X. Chen, L. Liu, Z. Liu, M.A. Marcus, W.C. Wang, N.A. Oyler, M.E. Grass, B. Mao, P.A. Glans, P.Y. Yu, J. Guo, S.S. Mao, Properties of disorder-engineered black titanium dioxide nanoparticles through hydrogenation, *Sci. Rep.* 3 (2013) 1–7. <https://doi.org/10.1038/srep01510>.
- [18] T. Wang, W. Li, D. Xu, X. Wu, L. Cao, J. Meng, A novel and facile synthesis of black TiO₂ with improved visible-light photocatalytic H₂ generation: Impact of surface modification with CTAB on morphology, structure and property, *Appl. Surf. Sci.* 426 (2017) 325–332. <https://doi.org/10.1016/j.apsusc.2017.07.153>.
- [19] J. Gao, Q. Shen, R. Guan, J. Xue, X. Liu, H. Jia, Q. Li, Y. Wu, Oxygen vacancy self-doped black TiO₂ nanotube arrays by aluminothermic reduction for photocatalytic CO₂ reduction under visible light illumination, *J. CO₂ Util.* 35 (2020) 205–215. <https://doi.org/10.1016/j.jcou.2019.09.016>.
- [20] J. Ge, G. Du, A. Kalam, X. Bi, S. Ding, Q. Su, B. Xu, A.G. Al-Sehemi, Oxygen vacancy-rich black TiO₂ nanoparticles as a highly efficient catalyst for Li–O₂ batteries, *Ceram. Int.* 47 (2021) 6965–6971. <https://doi.org/10.1016/j.ceramint.2020.11.045>.
- [21] Y. Yang, W. Shi, S. defect-engineered T. nanocrystals fabricated through square-wave alternating voltage as high-performance anode materials for lithium-ion batteries Liao, R. Zhang, S. Leng, Black defect-engineered TiO₂ nanocrystals fabricated through square-wave alternating voltage as high-performance anode materials for lithium-ion batteries, *J. Alloys Compd.* 746 (2018) 619–625. <https://doi.org/10.1016/j.jallcom.2018.02.309>.
- [22] S. Li, Y. Song, Y. Wan, J. Zhang, X. Liu, Hierarchical TiO₂ nanoflowers percolated with carbon nanotubes for long-life lithium storage, *J. Electroanal. Chem.* 934 (2023) 117305. <https://doi.org/10.1016/j.jelechem.2023.117305>.
- [23] K.M. Naik, E. Higuchi, H. Inoue, Electrocatalytic performances of oxygen-deficient titanium dioxide nanosheet coupled palladium nanoparticles for oxygen reduction and hydrogen evolution reactions, *Int. J. Hydrogen Energy* 48 (2023) 30741–30750. <https://doi.org/10.1016/j.ijhydene.2023.04.263>.

- [24] G. Liu, W. Li, R. Bi, C. Atangana Etogo, X.Y. Yu, L. Zhang, Cation-Assisted Formation of Porous TiO_{2-x} Nanoboxes with High Grain Boundary Density as Efficient Electrocatalysts for Lithium-Oxygen Batteries, *ACS Catal.* 8 (2018) 1720–1727. <https://doi.org/10.1021/acscatal.7b04182>.
- [25] B. Li, Y. Jiang, J. Liu, K. Hui, L. Guo, Photocatalytic and electrocatalytic activity of black TiO₂ nanotube arrays by aluminothermic reduction, *Micro Nano Lett.* 18 (2023) 1–5. <https://doi.org/10.1049/mna2.12152>.

Open Access This chapter is licensed under the terms of the Creative Commons Attribution-NonCommercial 4.0 International License (<http://creativecommons.org/licenses/by-nc/4.0/>), which permits any noncommercial use, sharing, adaptation, distribution and reproduction in any medium or format, as long as you give appropriate credit to the original author(s) and the source, provide a link to the Creative Commons license and indicate if changes were made.

The images or other third party material in this chapter are included in the chapter's Creative Commons license, unless indicated otherwise in a credit line to the material. If material is not included in the chapter's Creative Commons license and your intended use is not permitted by statutory regulation or exceeds the permitted use, you will need to obtain permission directly from the copyright holder.

